# Calculations of Long Pulsed Lasers for Lithotripsy

**Murooj N. Mohammad Ali***

Received on:1/9/2010
Accepted on:2/12/2010

**Abstract**

Urinary stone fragmentation with long pulsed Ho:YAG laser (wave length equal 2.1 µm) and Er:YAG laser (wave length equal 2.94 µm) investigated in this paper.

Fragmentation efficiency of these two lasers is measured by using various energy settings. Laser induced crater depth and ablation volume for both lasers were examined and compared using mathematical model. Theoretical results were compared with experimental results obtained by Hyun Wook Kang.

The study shows that the theoretical results and experimental results are comparable, and the crater depth when using Er:YAG laser was more than that on Ho:YAG laser.

**Keywords:** Long Pulsed Lasers, Er:YAG laser, Ho:YAG laser.

## الحسابات للنبضات الليزرية الطويلة لتفتيت الحصاة

**الخلاصه**

في هذا البحث تم دراسة عملية تفتيت الحصاة في المسالك البولية باستخدام النبضات الطويلة، الهلوميوم ياك بالطول الموجي 2.1 µm والايربيوم ياك بالطول الموجي 2.94µm .
وحساب كفاءة التفتيت او التكسير لنوعي الليزر المستخدمة وبطاقات مختلفة. ومقارنة عمق وحجم الحفر الليزري المؤثر لنوعي الليزر المستخدمين باستعمال النموذج الرياضي. تناولنا دراسة النموذج النظري والنتائج لهذا النموذج ومقارنته مع النتائج المختبرية المستحصلة من قبل الباحث Hyun Wook Kang .
الدراسة بينت ان النتائج المستحصلة من النموذج الرياضي قابلة للمقارنة مع النتائج المختبرية، وتبين ان التكسير الحجمي والحفر باستعمال ليزر الايربيوم هو اكبر من استعمال ليزر الهولوميوم.

## 1- Theory

There are many different mechanisms through which laser light can interact with stone, and these have been categorized in a number of different ways. The most common interaction mechanisms for therapeutic and surgical applications are : photothermal ablation and photomechanical/photoacoustical ablation.[1]

The Ho:YAG laser is a solid state, pulsed laser that emits light at 2.1 µm. the ability to fragment all stone into tiny fragments that are easily passed with little risk of ureteral obstruction[2].

The pulse duration in lithotripsy of the holmium laser ranges from (250-350) µsec., pulse energy from (0.2-4.0) J/pulse, frequency from (5-45) Hz and the average power from (30–80) watts. The version that one chooses will depend on the intended application. Light at the 2.1 µm wavelength is invisible to the human eye and falls in the near-infrared

* Electromechanical Engineering Department, University of Technology/Baghdad

region of the electromagnetic spectrum [2].

The Er:YAG laser operates at a wavelength of 2.94 µm at 20°C and a pulse duration in lithotripsy of ( 250-300 ) µsec. the Er:YAG laser application is 2.25 W potency, 11 mm focal distance, 4 Hz frequency, 0.2 J/pulse energy; 62 J total energy and 313 mean impulse[3]. The applications of Er:YAG is an excellent choice for Medical Laser Systems, and dental laser systems.

## 2- Unification of Blow-off and Steady-state Models

The basis of steady-state ablation is that a certain amount of energy (heat of ablation) must be supplied to the stone before ablation can begin.

The absorption coefficient determines the spatial distribution of the energy, and hence, the time necessary for a given ablation threshold to be reached. If the heat of ablation is delivered to the stone during the laser pulse, material ejection begins, and all of the laser energy following this point will be used to drive an ablation front that moves into the stone at a constant velocity, until the end of the laser pulse. In the traditional steady-state model, it is assumed that the ablated material is removed instantaneously and no longer plays a role in the ablation process [4].

However, a more realistic scenario is that once the ablation threshold is reached, material is ejected from the stone surface and interacts with the incident beam. If the ablation begins early enough during the incident laser pulse, the plume of ejected particles may obscure the incident beam, and attenuate the beam by absorbing the laser radiation [5]. By assuming that the screening of the incident laser beam follows a Beer's law distribution in the plume:

$$E(z) = E_0 e^{-\gamma z} \quad \ldots\ldots (1)$$

Where z : Certain depth (cm).

where E(W/mm2) laser beam irradiance, γ (mm-1) is the plume attenuation coefficient. By applying equation (1) to the source term for a one dimension heat equation and neglecting heat diffusion, one can derive an expression for the ablation depth[6,7]:

$$d = \frac{1}{\gamma} \ln\left[\frac{\gamma}{\mu_a}\left(\frac{H_0}{H_{th}} - 1\right) + 1\right] \quad (2)$$

Where Ho : Incident laser radiant exposure (J/cm2).

Hth : Threshold laser radiant exposure (J/cm2).

$\mu_a$ : Absorption coefficient (cm -1).

If multiple laser pulses (n) are used to reate an ablation crater, the total crater depth becomes:

$$d = \sum_{i=1}^{n} \frac{1}{\gamma} \ln\left[\frac{\gamma}{\mu_a}\left(\frac{H_i}{H_{th}} - 1\right) + 1\right] \quad (3)$$

Where Hi : Laser radiant exposure for multiple pulses (J/cm2).

This assumes that successive laser pulses are sufficiently far apart in time so that ejects from the previous pulse do not screen the current pulse [6, 7].

However, if plume attenuation is not negligible, then assume the plume attenuation coefficient γ to be proportional to the stone absorption coefficient µa since the material composition of the ejector should be the same as the unablated stones [4, 5].

Furthermore, we expect $\gamma << \mu a$ since much of the plume consists of

vapor with a much lower density than the native tissue. With these assumptions, substitute $\gamma = \beta\mu a$, $\beta$ should be << 1 to get the condition $\gamma << \mu a$, into equation (2) to arrive at a modified form of the ablation depth model [6]:

$$d = \frac{1}{\beta\mu_a}\ln\left[\beta\left(\frac{H_0}{H_{th}}-1\right)+1\right] \quad \ldots(4)$$

where $\beta$ is proportionality constant.

In this case, as the astone absorption coefficient rises, the increasing plume attenuation coefficient causes the ablation depth to plateau. As the absorption coefficient rises further, the plume attenuation coefficient (seen here as $\beta$) asserts a stronger effect, and begins to decrease the ablation depth as more of the laser pulse energy is attenuated [4, 6, 7].

**3- Calculations:**

The volume of urinary stone that is vaporized by the excess of one laser pulse energy above threshold can be estimated by multiplying equation (2) by the area of the laser spot size (A):

$$V_{vaporized} = \frac{A}{\gamma}\ln\left[\frac{\gamma}{\mu_a}\left(\frac{H_0}{H_{th}}-1\right)+1\right] \quad \ldots(5)$$

If multiple laser pulses (N) are employed to achieve sufficient ablation effect, the total ablation volume will be:

$$V_{vaporized} = \sum_{i=1}^{N}\frac{A}{\gamma}\ln\left[\frac{\gamma}{\mu_a}\left(\frac{H_i}{H_{th}}-1\right)+1\right] \ldots(6)$$

To evaluate the relation between ablation volume or depth and the pulse duration, the simple equation which connects the pulse duration and energy as used is:

$$E = P.\tau p \quad \ldots\ldots\ldots\ldots(7)$$

where $\tau p$ is the pulse duration in (s) and P is the peak power in (W). The threshold radiant exposure gets from:

then:

$$H_{th} = \frac{E}{A} \quad \ldots\ldots\ldots\ldots(8)$$

$$H_{th} = \frac{P.\tau_p}{A} \quad \ldots\ldots\ldots\ldots(9)$$

The following relations for crater depth and ablation volume are achieved by substituting equation (9) into equations (2) and (5):

$$d = \frac{1}{\gamma}\ln\left[\frac{\gamma}{\mu_a}\left(\frac{A.H_0}{P.\tau_p}-1\right)+1\right] \ldots(10)$$

$$V = \frac{A}{\gamma}\ln\left[\frac{\gamma}{\mu_a}\left(\frac{A.H_0}{P.\tau_p}-1\right)+1\right] \ldots(11)$$

The absorption coefficient of each stone for Ho:YAG and Er:YAG can be calculated by using equation (12) as[6]:

$$H_{th} = \frac{1}{\mu_a}\left[\rho\left(c(T_0-T_{th})+L\right)\right] = \frac{W_{abl}}{\mu_a} \ldots(12)$$

$$\mu_a = \frac{1}{H_{th}}\left[\rho\left(c\Delta T + L\right)\right] \ldots(13)$$

The parameters which are necessary to substitute in the mathematical models are shown in Table (1).

**4- Results:**

**a- Crater volume**

Figure (1) compare between the results of calculating the crater volume as a function of incident radiant exposure for single pulse Ho:YAG laser and Er:YAG laser-

COM stone . This figure presents both the experimental results and unification model results. Crater volume when use Er:YAG laser is more than that when use Ho:YAG laser in both experimental and theoretical results.

Figure (2) show the crater volume as a function of incident radiant exposure Ho:YAG laser and Er:YAG laser-COM stone . This figure presents both the experimental results and unification model results under the effect of five laser pulses. Crater volume when use Er:YAG laser increase about three times that when use Ho:YAG laser but on Ho:YAG laser the experimental and theoretical results was comparable more than that of Er:YAG laser.

Figure (3) compare between The crater volume as a function of pulse duration for Ho:YAG and Er:YAG laser-COM stone by applying equation (13). As pulse duration increase crater volume decrease when use both lasers.

Figure (4) compare between The calculation results as a function of multiple Ho:YAG laser pulses and Er:YAG laser on COM stone by applying equation (8). As number of pulses increase the ablation volume increase.

**b- Crater depth**

Figure (5) compare between the results of calculating the crater depth as a function of incident radiant exposure for single pulse Ho:YAG laser and Er:YAG laser on COM stone . This figure presents both the experimental results and unification model results. The depth created by Er:YAG laser is more than that created by Ho:YAG in both experimental and theoretical results. But on Ho:YAG laser the experimental and theoretical results were close than that on Er:YAG laser.

Figure (6) show the crater depth as a function of incident radiant exposure Ho:YAG laser and Er:YAG laser on COM stone . This figure presents both the experimental results and unification model results under the effect of five laser pulses. On figure (6) the crater depth of Er:YAGis about four times that occurred by Ho:YAG laser in both theoretical and experimental results, but on Ho:YAG laser the experimental results and theoretical was more comparable than the results obtained by using Er:YAG laser.

Figure (7) compare between The crater depth as a function of pulse duration for Ho:YAG and Er:YAG laser on COM stone by applying equation (12). The crater depth on both lasers are inversely proportional with pulse duration.

Figure (8) compare between The calculation results as a function of multiple Ho:YAG laser pulses and Er:YAG laser on COM stone by applying equation (3). As number of pulses increase crater depth also increase.

**5- Discussion**

One of the sources of the small differences between the mathematical and practical results is due to the collection of different parameter values for the mathematical model from different references; beside the model consider only one laser–stone interaction phenomenon, while the experimental results are based on real application of laser to the stone.

The theoretical results and experimental results for two types of lasers are comparable. The ablation volume crater depth when using

Er:YAG laser was more than that on Ho:YAG laser because the absorption coefficient of COM stone in Er:YAG laser (μa COM) is much more than the absorption coefficient of (μa COM) COM stone in Ho:YAG laser, so that Ho:YAG laser introduced a shelling operation on the stone but in Er:YAG laser were introduced a drilling operation on the stone , so the Ho:YAG laser favorite on laser lithotripsy. The pulse duration governs the dominant mechanism in calculi fragmentation, which is either photo thermal or photo acoustical. Lasers with long pulse durations induce a temperature rise in the laser-affected zone with minimal acoustic waves, material is removed by means of vaporization, melting, mechanical stress, and chemical decomposition. Short-pulsed laser ablation, on other hand, produces shock waves, and the resultant mechanical energy fragments calculi.

**References**

[1] Widian H.R., "*Modeling of Laser Lithotripsy Technique"*, M.sc. thesis, Baghdad, 2008.

[2] Lt Col AS Sandhu, Lt Col A Srivastava, Maj Gen P Madhusoodanan, Col T Sinha, Lt Col SK Gupta, Wg Cdr A Kumar, Wg Cdr GS Sethi, Lt Col R Khanna, "*Holmium:YAG Laser for Intracorporeal Lithotripsy*", MJAFI; 63 : 48-51, 2007.

[3]Tanji EY, Matsumoto K, Eduardo CP. *Scanning electron microscopic observations of dentin surface conditioned with the Er:YAG laser*. Deuts Gesellschaft Laser Newsletter 1997.

[4]AlfredVogel, Vasan Venugopalan, "*Mechanisms of Pulsed Laser Ablation of Biological Tissues*", Chemical Reviews, Vol. 103, No. 2, American Chemical Society ©2003.

[5] Kin Foong Chan, Bernard Choi, Gracie Vargas, Daniel X. Hammer, Brian Sorg, T. Joshua Pfefer, Joel M. H. Teichman, Ashley J. Welch, E. Duco Jansen, "*Free Electron Laser Ablation of Urinary Calculi: An Experimental Study*", IEEE Journal on Selected Topics in Quantum Electronics, Vol. 7, NO. 6, November/December 2001.

[6] Stephen R. Uhlhorn, "*Free Electron Laser Ablation of Soft Tissue: The Effects of Chromophore and Pulse Characteristics on Ablation Mechanics*", Ph.D. Thesis, Department of Biomedical Engineering, Vanderbilt University, August 2002.

[7] Joseph A. Izatt, Norris D. Sankey, Firooz Partovi, Maryanne Fitzmaurice, Richard P. Rava, Irving Itzkan, and Michael S. Feld, "*Ablation of Calcified Biological Tissue Using Pulsed Hydrogen Fluoride Laser Radiation*", IEEE Journal of Quantum Electronics, vol. 26. NO. 12, December 1990.

[8] Z.X. Jiang, C. Whitehurst, T.A. King, "*Basic Mechanisms in Laser Lithotripsy.1: Optoacoustic-mechanical Analysis"*, Lasers in Medical Science Vol. 6:443, Baillière Tindall ©1991.

[9] Hyun Wook Kang, B.S.M.E.; M.S.M.E., "*Enhancement of High Power Pulsed Laser Ablation and Biological Hard Tissue Applications"*, Ph.D. Thesis, University of Texas at Austin, December 2006.

**Table (1) Physical parameters of calcium oxalate monohydrate COM stone**

| Arameter | Symbol | Value | Unit | Ref |
|---|---|---|---|---|
| Temperature rise required for ablation | $\Delta T$ | 596 | K | [8] |
| Latent heat of vaporization | L | 2580 | J/g | 4] |
| Laser number of pulses | N | 5-50 | - | Chosen |
| Density of COM | $\rho_{(COM)}$ | 2.224 | $g/cm^3$ | [8] |
| Threshold radiant exposure of COM in $\lambda$=2.1 μm | $H_{th(COM)}$ | 7.4 | $J/cm^2$ | [6] |
| Specific heat of COM | $c_{(COM)}$ | 1 | J/(g.K) | [8] |
| Threshold Radiant Exposure of COM in $\lambda$=2.9 μm | $H_{th(COM)}$ | 0.4 | $J/cm^2$ | [6] |
| Absorption coefficient of COM in Ho:YAG laser | $\mu_{a(COM)}$ | 700 | $cm^{-1}$ | Calculated |
| Absorption coefficient of COM in Er:YAG laser | $\mu_{a(COM)}$ | 1250 | $cm^{-1}$ | Calculated |

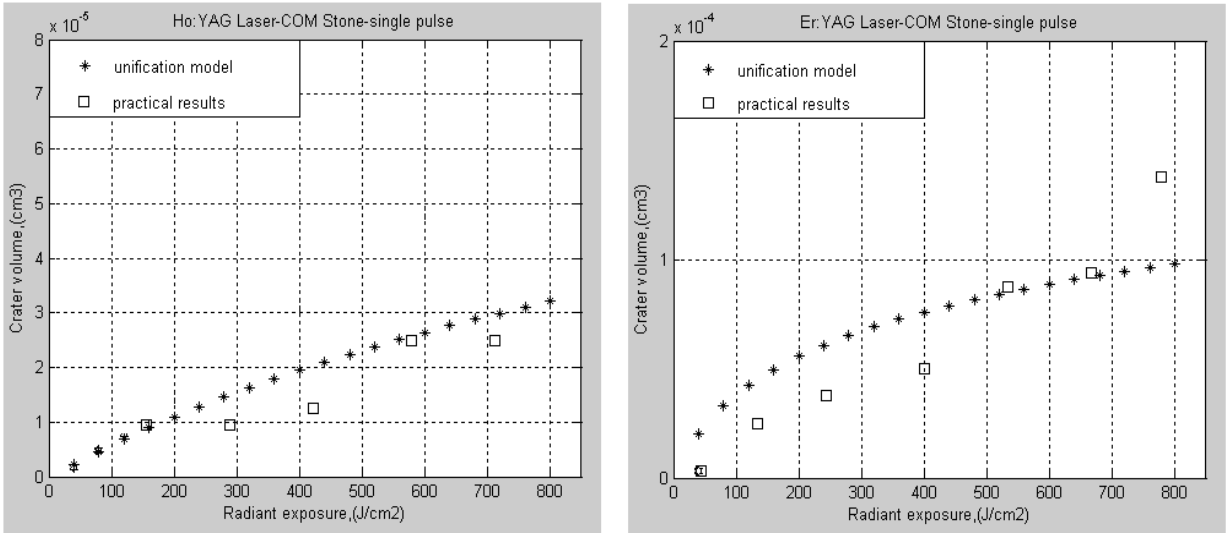


**Figure (1): Crater volume with respect to radiant exposure for Ho: and Er:YAG laser-COM stone – single pulse**

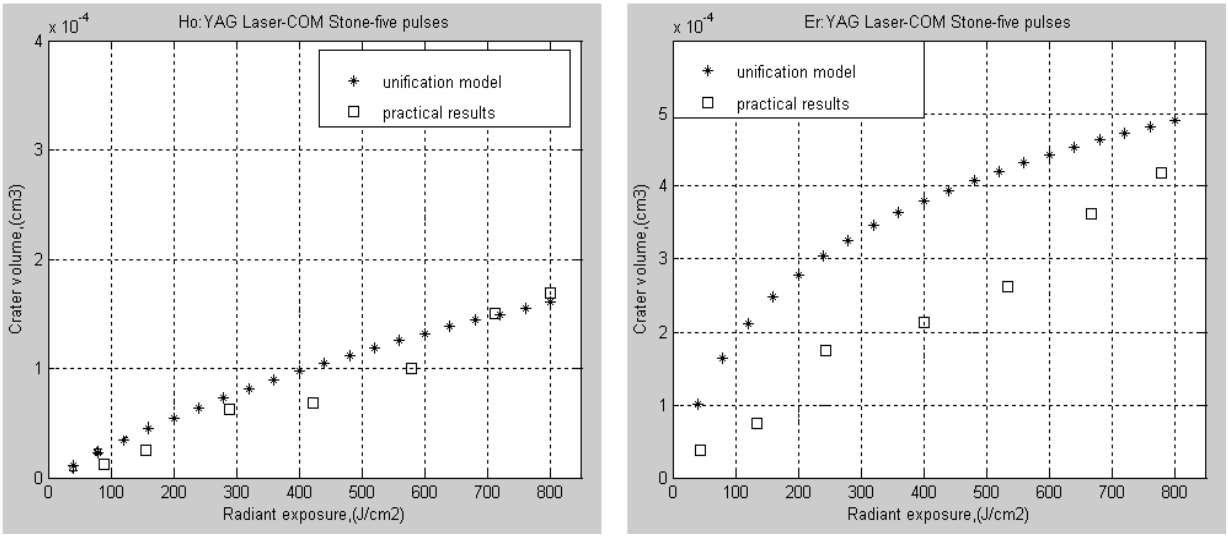


**Figure (2): Crater volume with respect to radiant exposure for Ho: and Er:YAG laser-COM stone – five pulses**

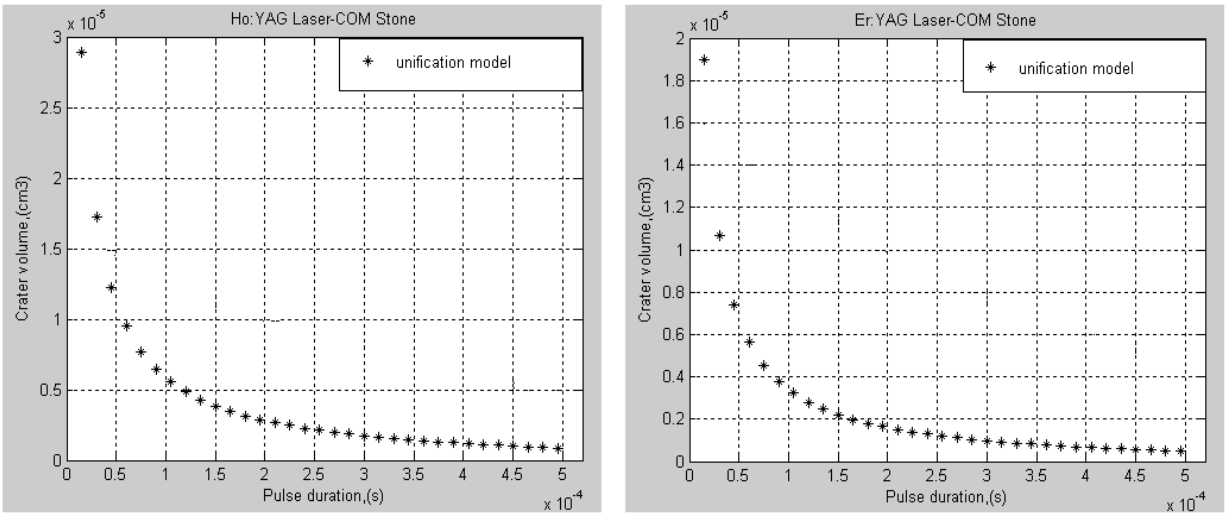


**Figure(3): Crater volume with respect to Pulse duration for Ho: and Er:YAG laser-COM stone**

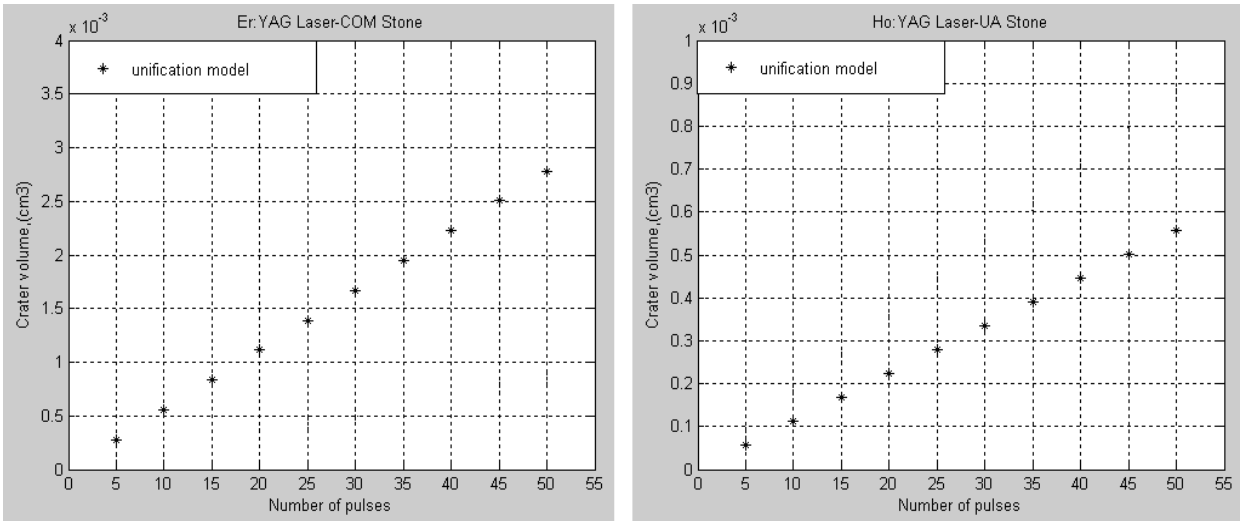


**Figure (4): Crater volume with respect to number of pulses for Ho: and Er:YAG laser-COM stone**

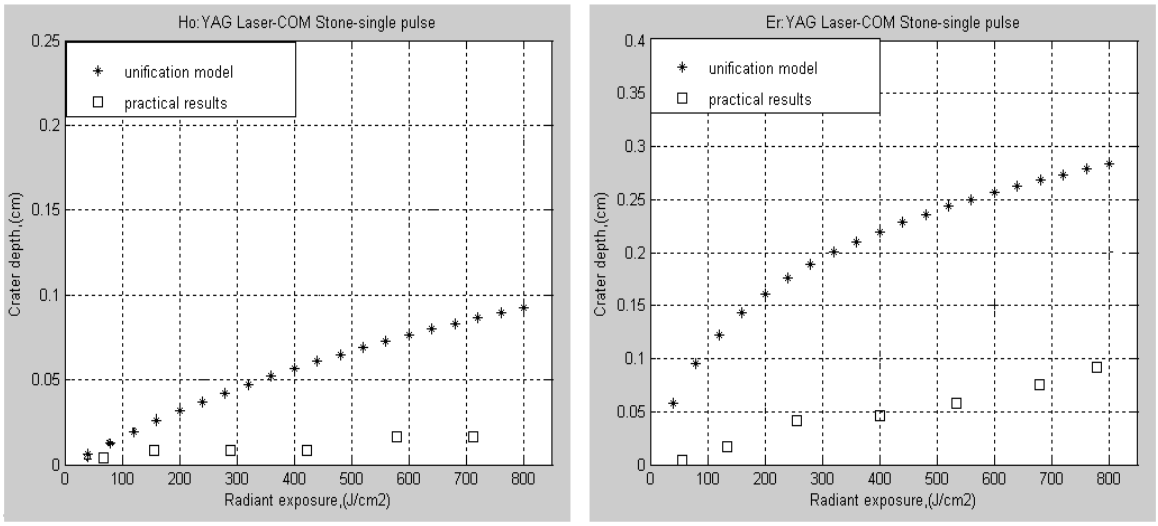


**Figure (5): Crater depth with respect to radiant exposure for Ho: and Er:YAG laser-COM stone – single pulse**

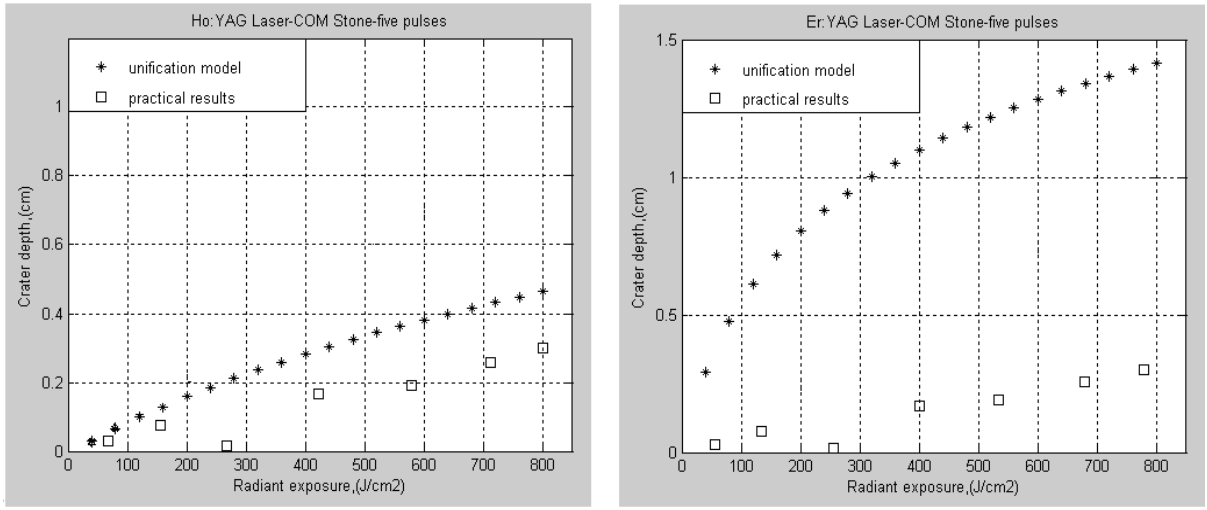


**Figure (6): Crater depth with respect to radiant exposure for Ho: and Er:YAG laser-COM stone – five pulses**

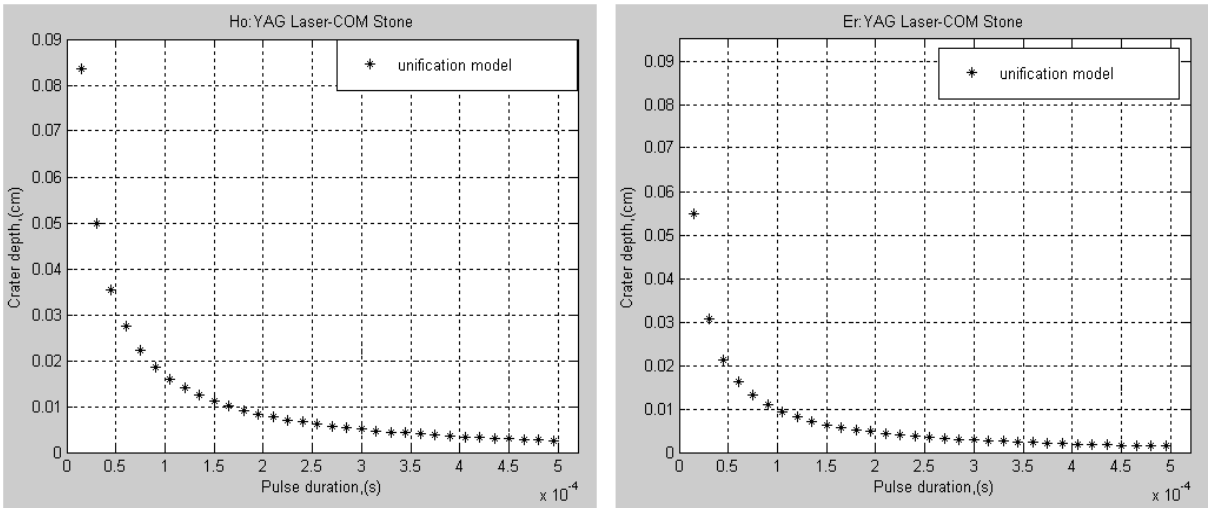


**Figure (7): Crater depth with respect to Pulse duration for Ho: and Er:YAG laser-COM stone**

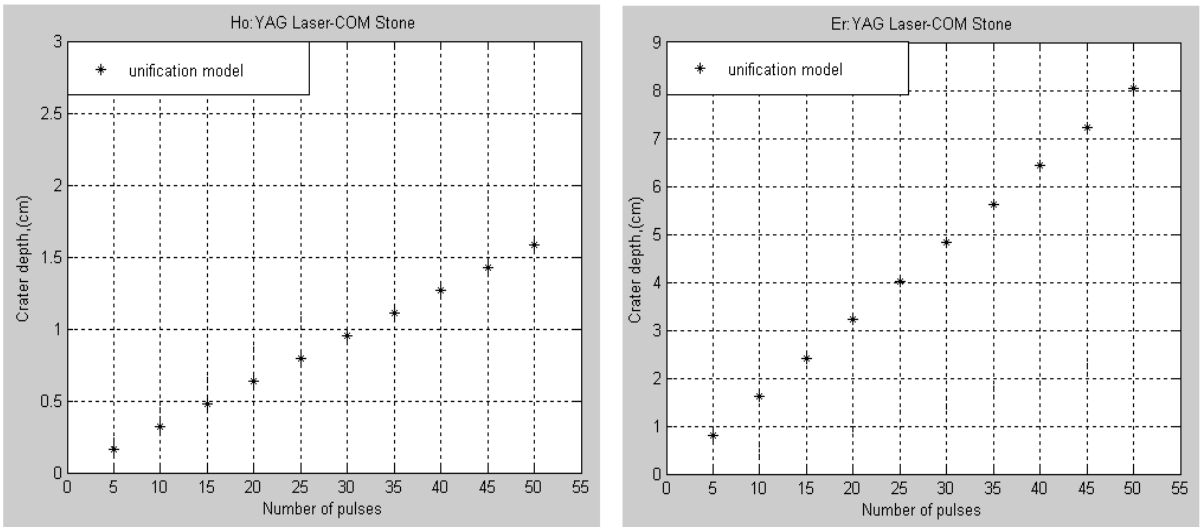


**Figure(8): Crater depth with respect to number of pulses for Ho: and Er:YAG laser-COM stone**